Appl Nanosci (2011) 1:37–44
DOI 10.1007/s13204-011-0005-4

ORIGINAL ARTICLE

Photocatalytic activities of wet oxidation synthesized ZnO and ZnO–TiO_2 thick porous films

Ruiqun Chen · Jie Han · Xiaodong Yan · Chongwen Zou · Jiming Bian · Ahmed Alyamani · Wei Gao

Received: 18 March 2011 / Accepted: 28 March 2011 / Published online: 20 April 2011

Abstract Highly porous zinc oxide (ZnO) film was produced by using reactive magnetron sputtering zinc target followed by wet oxidation. Titanium dioxide (TiO_2) was mixed to the porous films by using either TiO_2 target magnetron sputter deposition or sol-spin method. The film thickness could reach 50 μm with uniform porosity. On the sputtering prepared ZnO–TiO_2 film surface, fine nanorods with small anatase TiO_2 nano-clusters on the tips were observed by SEM and TEM, and the titanium (Ti) composition was determined by XPS as 0.37%. The sol-spin treatment could increase the Ti composition to 4.9%, with reduced pore size compared to the untreated ZnO porous film. Photoluminescence measurements showed that the Ti containing porous film has strong ultraviolet-visible light emission. In the photo-catalysis testing, ZnO and ZnO–TiO_2 have similar photo-catalysis activity under 365 nm UV irradiation, but under visible light, the photocatalysis activities of ZnO–TiO_2 films were twice higher than that of ZnO porous film, implying promising applications of this porous oxide composite for industrial and dairy farm wastewater treatment.

Keywords Zinc oxide · Titanium dioxide · Porous film · Reaction with estrone · Photocatalysis with visible light

Introduction

Titanium dioxide (TiO_2) and zinc oxide (ZnO) are both intensively studied for photo-electro-chemical applications such as photocatalysis and dye sensitized solar cells (DSSC). In comparison, TiO_2 has large band-gap energy of 3.2 eV (Mardare et al. 2000) for anatase phase and 3.0 for rutile phase (Lee et al. 2006), similar to ZnO, but it is more environmental-resistant than ZnO. Anatase phase has been commercially used as photocatalyst due to its good performance. However, synthesis of TiO_2 nanostructure is high-energy consuming process. The most commonly used method to synthesize TiO_2 nanostructures is vapour–liquid–solid (VLS) method, which requires working temperature over 1,000°C (Lee et al. 2006; Wu et al. 2005). Moreover, TiO_2 nanostructures produced by the thermal method are mostly in rutile phase, which is not as good as anatase phase for photo-electro-chemical applications. The common methods to produce anatase phase TiO_2 nanostructures and porous films are chemical processes, such as chemical template synthesis (Hulteen and Martin 1997), anodic oxidation of Ti foil (Gong et al. 2001), alkaline hydrothermal method (Bavykin et al. 2006) and doctor

R. Chen and J. Han contributed equally to the work.

R. Chen (✉) · J. Han · X. Yan · C. Zou · W. Gao (✉)
Department of Chemical and Materials Engineering,
University of Auckland, 20 Symonds Street,
Private Bag 92019, Auckland 1142, New Zealand
e-mail: rche058@aucklanduni.ac.nz

W. Gao
e-mail: w.gao@auckland.ac.nz

C. Zou
National Synchrotron Radiation Laboratory,
University of Science and Technology of China,
Hefei 230026, China

J. Bian
School of Physics and Optoelectronics Engineering,
Dalian University of Technology, Dalian 116024, China

A. Alyamani
National Center for Nanotechnology Research,
King Abdulaziz City for Science and Technology,
P.O. Box 6086, Riyadh 11442, Saudi Arabia

blade method (Luque and Hegedus 2003). In addition, TiO_2 also has low electron mobility, which is one of the key factors that limited the efficiency of DSSC using TiO_2 as the electrodes (Zou et al. 2009; Hsu et al. 2007).

On the other hand, ZnO is a semiconductor material with a wideband gap of 3.37 eV and high exciton energy of 60 meV at room temperature (Vogel et al. 1995). Its easy formation of various nanostructures and high electron mobility make many researchers believe it can help to further increase the working efficiencies of current used TiO_2 based products (Hsu et al. 2007). Therefore, using ZnO–TiO_2 porous film can be the way of combining the advantages of both materials to achieve this goal.

For both photocatalysis and DSSC applications, high surface area is advantaged for performance with high efficiency. In catalysis applications, the use of either nanopowders or porous film can achieve high surface area, but the supported porous film has the advantages of reusable and reducing the secondary contamination over nanopowders.

The most commonly used techniques to produce ZnO porous film are chemical methods, such as electrochemical deposition (Xi et al. 2008), (Gan et al. 2009), (Liu et al. 2009), which needs chemical reagents direct the deposition orientation to achieve porosity. It requires chemical waste treatment to address the environment issues. We report another physical-chemical approach of using reactive sputtering and wet oxidation to produce ZnO film with consistent porosity and high thickness. This method is free of use of chemical and time-effective. ZnO porous film mixed with TiO_2 can be produced by this method.

Experimental procedure

Partially oxidized Zn films on glass substrates were prepared by a magnetron sputtering (MS) system with a Zn target (99.99% Zn). On the sputtering stage, a TiO_2 target (99.99% TiO_2) could be installed 180° to the Zn target (in the opposite position as the Zn target) to mix TiO_2 into the partially oxidized Zn film. A mixture of Ar and O_2 (8:2 vol.) was introduced into the chamber as the working gas with the total pressure of 10 mTorr. The deposition time is 30 min. The films were then taken out and oxidized in a tube furnace with a wet O_2 flux at 450°C for 1 h to produce porous ZnO film and Type-1 ZnO–TiO_2 film (ZnTiO-1).

After the oxidation treatment, some of the produced ZnO porous films were immersed in the TiO_2 sol and placed under UV irradiation for 2 h, so that the TiO_2 sol could thoroughly seep into the pores of the films. ZnO films exhibit strong hydrophilic properties under UV irradiation, which is helpful for the TiO_2 absorption into the films. The film was then spun at 6,000 rpm for 30 s to remove the extra sol, and followed by annealing at 450°C for 1 h to crystallize TiO_2 and produced type-2 ZnO–TiO_2 film (ZnTiO-2).

The morphologies and microstructure of surface and cross section of the films were examined with scanning electron microscopy (FEG-SEM, Philips XL-30S). The phase analysis was conducted by using X-ray diffractometry (Druker D8, Cu-Kα radiation). The diffuse reflectance test (Shimadzu 2100 UV/vis) was adopted to obtain the absorption spectra of the porous films. $BaSO_4$ was used as a reference for all test samples. Optical properties were also measured by photoluminescence (PL) with a 325 nm laser source. The crystal structure was studied with a high-resolution transmission electron microscope (HRTEM).

The performances of ZnO and ZnO–TiO_2 porous films as photocatalysts were then tested on degrading estrone under UV, visible and UV-visible (VIS) light sources. Estrone was chosen as the candidate is because that estrone belongs to the group of estrogen which is one of the endocrine disrupting chemicals (EDC). It has been detected in wastewater treatment plant effluent and can affect environments biologically with even a very low concentration. Therefore, the study of the degradation of estrone has more practical environmental significance than other commonly used dye chemicals in laboratory.

At the beginning of the degradation test, the catalyst films on the glass substrate with the dimension of 15 mm × 15 mm were immersed in 10 ml estrone aqueous solution with concentration of 0.3 ppm. The estrone solutions with catalyst films were kept in the dark for 30 min before exposure to light irradiation, which was long enough for the absorption of estrone into the films to reach equilibrium. So that the measured concentration changes during UV irradiation would be solely caused by photodegradation. An 18 W UV lamp ($\lambda = 365$ nm, Osram) was used as the UV only light source.

A 300 W UV-VIS lamp ($\lambda \geq 280$ nm, Osram ultravitalux) was used as UV-VIS light source, and the visible light was obtained by using a Kenko UV-filter to block the UV light from the UV-VIS lamp. The exposure time under light was 4 h. The distance from the film to the solution surface was fixed in all experiments to maintain a consistent attenuation factor for the incident light. The incident light intensity from the UV-Vis lamp on the solution surface was measured by a radiometer (IL1700, International Light, USA). A blank experiment without photocatalyst in the solution was conducted for each run as a reference. For each solution, 300 μL fluid was sampled at the time point of −30, 0, 30, 60, 120, 180, and 240 min, where 0 min is the starting point of light irradiation. The estrone concentration was tested by high performance liquid chromatography (HPLC, Agilent 1100 series).

Results and discussions

Crystal structures

The reactive sputtering deposition yielded partial oxidized Zn films. The XRD pattern (Fig. 1) shows both Zn and ZnO peaks with no preferential orientation. All Zn peaks were vanished after 1 h wet oxidation, indicating that the residual Zn has been transformed to ZnO. Figure 2a and b shows the surface and cross section morphology of the ZnO film. The cross section view shows the thickness of the film is about 50 μm; and the porosity is uniformly distributed throughout the thickness.

For the ZnTiO-1 film produced by reactive sputtering Zn and TiO_2 targets followed by wet oxidation treatment, there is no TiO_2 related peaks detected from the as-deposited Zn-TiO_2 film by XRD. The XRD pattern is similar to the one shown in Fig. 1 for ZnO porous film. This is probably because that the TiO_2 was not crystallized in as-deposited Zn-TiO_2 film. ZnTiO-1 film has similar film thickness with the ZnO porous film but the surface of the film was covered by short rods with nano-size cluster formed on the tips, shown in Fig. 2c and d.

After sol-spin treatment, the final porosity was retained in ZnTiO-2 (Fig. 2e, f), although it may have slightly decreased compared to the original ZnO porous film shown in Fig. 2a, b. The XPS analysis shows the Ti concentration is 4.9%.

The TEM image (Fig. 3a) shows that the cluster on the tip is polycrystalline. Another high-resolution TEM photo was taken on the grain boundary area (Fig. 3b). The lattice spacing of the two adjacent grains is 0.2377 nm (up-left) and 0.2430 nm (bottom-right), corresponding to the [004] and [103] planes of TiO_2 anatase phase, respectively. Therefore, the TEM result proves that the tip part of small clusters of the nanorod is TiO_2 in anatase phase. These TiO_2 nanoclusters could be formed by agglomeration of the amorphous TiO_2 that had been dispersed into the ZnO matrix at the sputtering stage, through thermal diffusion process during the wet oxidation. The wet oxidation temperature was 450°C. It has been reported that most of the amorphous TiO_2 can transform to the anatase state at temperature above 350°C after 1 h annealing (Baltazar et al. 2006), and the anatase–rutile transformation temperature is around 600°C (Masaru et al. 1997). This can also prove that the formed TiO_2 crystal is in the anatase phase not rutile. Although the SEM can only observe anatase nanoclusters on the surface, TiO_2 nanoparticles should also exist in the porous film. The reason that the XRD result did not show any TiO_2 anatase peak could be due to the quantity and the size of the TiO_2 being too low to be detected, and the Ti% detected by XPS is 0.39%.

Optical properties

Figure 4 illustrates the plots of the absorption curves of the ZnO porous film, film ZnTiO-1 and ZnTiO-2. The absorption edges of these three films are located between 370 and 390 nm.

However, the inserted plot shows that the optical gap (E_g) of the film ZnTiO-1 has a red-shifted from the ZnO porous film. The E_g of film ZnTiO-2 further red shifted

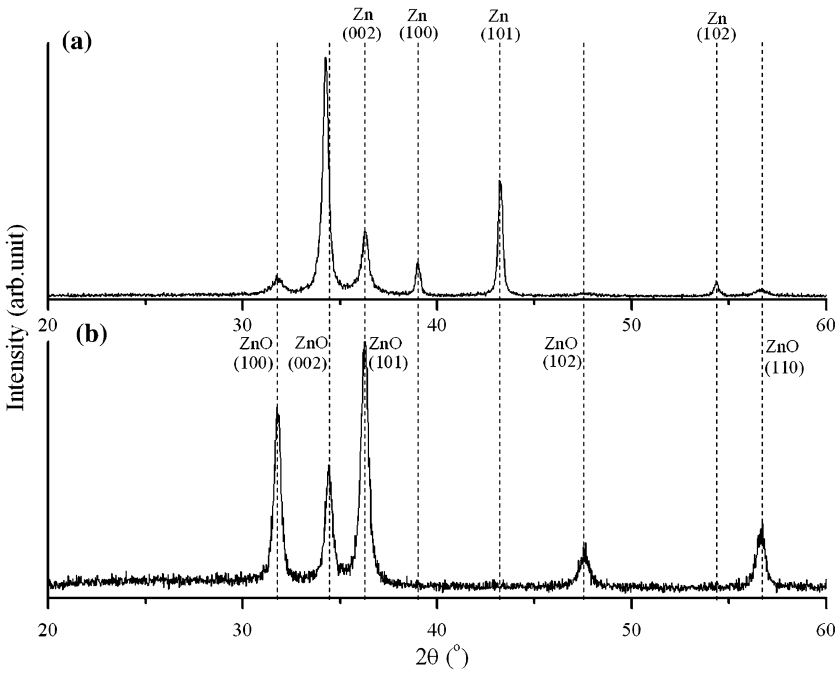

Fig. 1 XRD spectra of **a** partial oxidized Zn precursor film after reactive sputtering for 30 min, and **b** ZnO porous film after wet oxidation at 450°C for 1 h

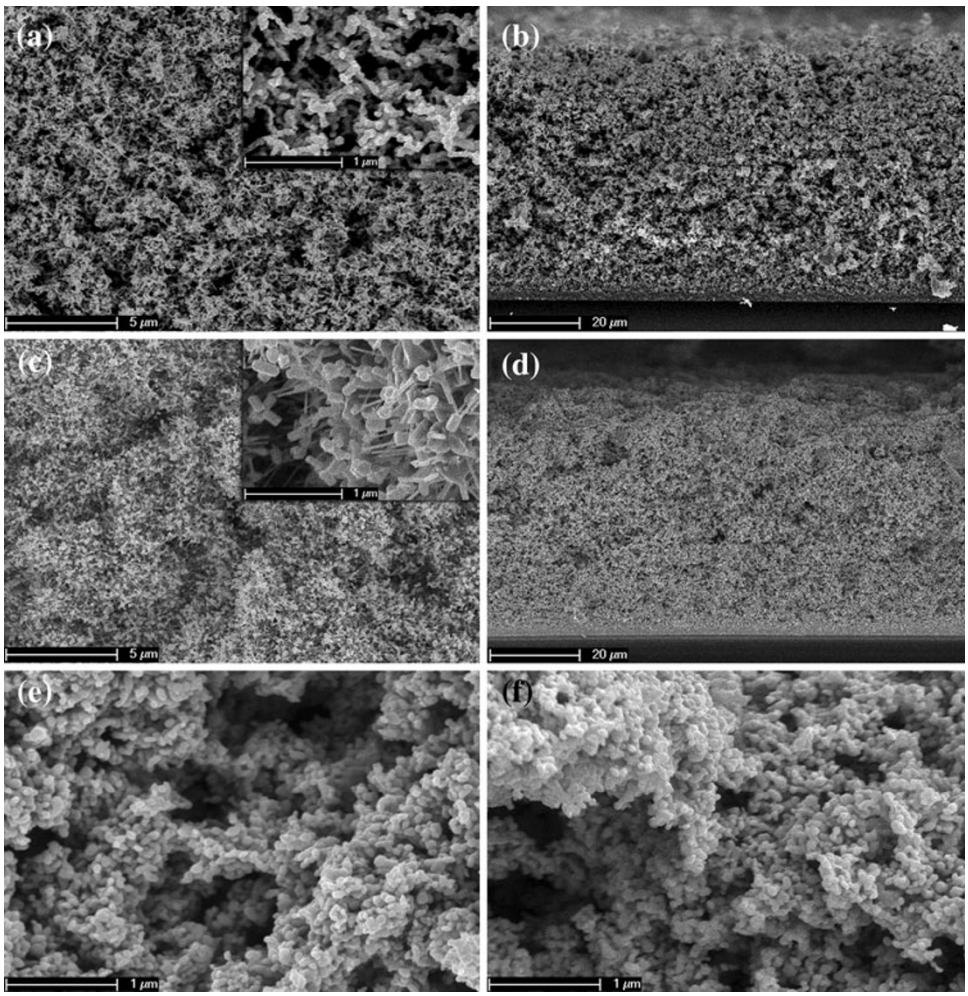

Fig. 2 SEM images of porous films after 1 hr wet-oxidation at 450°C: **a** top view of ZnO porous film, **b** cross section view of ZnO porous film, **c** top view of ZnTiO-1 film, **d** cross section view of ZnTiO-1 film, **e** top view of ZnTiO-2 film, and **d** cross section view of ZnTiO-2 film at high magnification

from film ZnTiO-1. These shifts can be attributed to the higher TiO_2 composition since TiO_2 has a smaller band gap than ZnO crystals

Figure 5 displays the room temperature PL spectrum of a porous ZnO film produced by wet oxidation, as well as a dense ZnO film deposited by MS. It is clear to see that the peak position of the porous ZnO PL spectrum is red shifted compared to the dense ZnO film (380 vs. 377 nm), which is mainly caused by the large surface area. The PL peak of the porous ZnO is also broader than the dense film, which should be resulted from the crystal quality and surface effect. The peak at 388 nm on the porous ZnO PL spectrum is believed to come from the system noise.

The results of PL measurement on ZnO-TiO_2 porous films are shown in Fig. 6. Both type ZnO–TiO_2 porous films have similar PL spectra characters, but only that the film ZnTiO-2 has stronger emission. The spectra show that the ZnO–TiO_2 porous films have a major light emission at 380–450 nm. The insert graph indicates that the curve can be deconvoluted into several peaks at 383, 393, 404, 412, 424, 434 and 450 nm. The peak at 383 nm is from ZnO (Choi et al. 2009), and the peak at 393 nm coincides with the E_g of anatase phase TiO_2 crystals (3.18 eV/390 nm (Nakajima et al. 2005), and 3.20 eV/387 nm (Mardare et al. 2000).

For the three peaks located at 404, 412 and 424 nm, there is no clear explanation of their origins, as in different literatures each of these three peaks has been explained by using the same origin: self-trapped excitons localized at TiO_6 octahedral sites (404 nm (Choi et al. 2009), 412 nm (Saraf et al. 1998), 424 nm (Lei et al. 2001)). However, these three peaks appear together from the ZnO–TiO_2 samples, probably indicating the enhanced self-trapped excitons induced by the combination of ZnO.

The other longer wave peaks could be attributed to the oxygen vacancies and the surface states (Lei et al. 2001; Zou et al. 2009). It is interesting to note that the light emission from ZnO is weaker compared to that from TiO_2, despite of the ZnO quantity is much greater than TiO_2. This phenomenon may be well explained by the recently reported coupling mechanism (Zou et al. 2009). According to Zou's explanation, the TiO_2 nano-clusters on the film surface may have absorbed some of the photons emitted from ZnO, and the TiO_2 nano-clusters were thus excited by

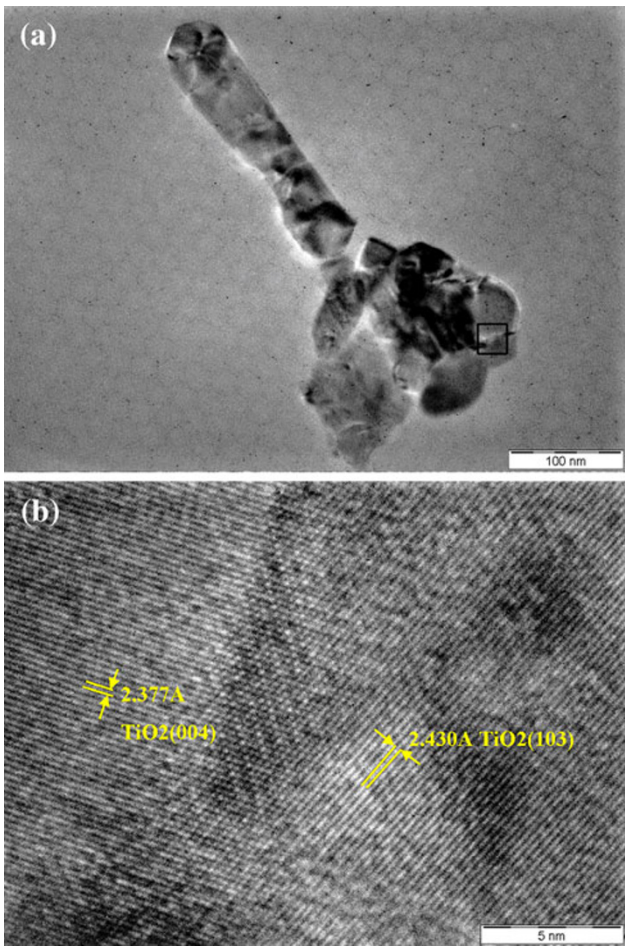

Fig. 3 **a** TEM image of a cluster structure on the film surface, and **b** the HRTEM image taken at the *boxed area* of **a**

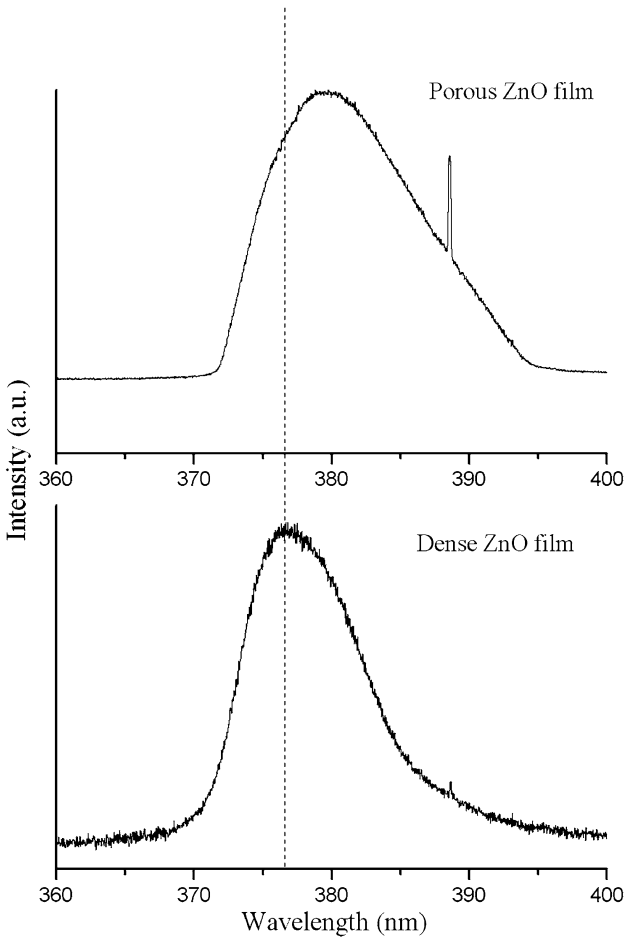

Fig. 5 The room temperature PL spectra of porous and dense ZnO films at the UV region with a 325 nm laser radiation source

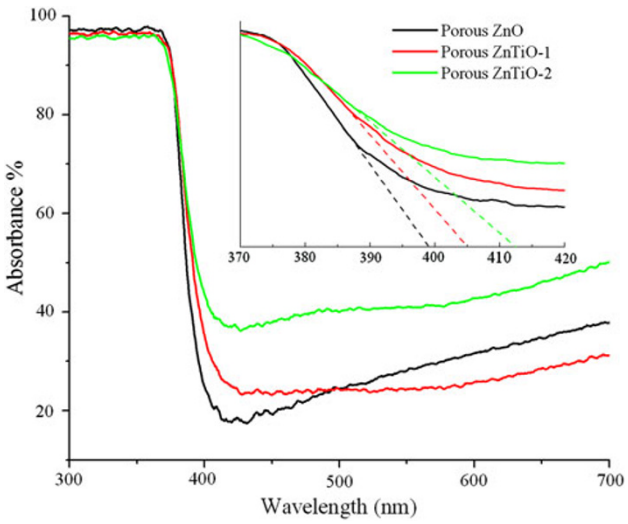

Fig. 4 The UV-VIS absorbance spectra of ZnO, ZnTiO-1, and ZnTiO-2 porous films

both the laser light and UV emission from the ZnO. This so-called "resonant effect" for the PL process may be the reason that the TiO_2 related peaks are more intensive than ZnO. The enhanced PL property suggests that these ZnO-TiO_2 composite films may have good performance in the photocatalysis applications such as DSSC, organic compounds decomposition, and water splitting for hydrogen productions.

Photocatalysis test

UV degradation

The photocatalytic performance of ZnO and ZnO–TiO_2 porous films was firstly tested by experiments of degrading estrone under UV light source.

Figure 7 displays the test results. The C/C_O on the *Y*-axis represents the ratio of the measured estrone concentration at each sampling time point to the original concentration. The estrone concentration of the blank

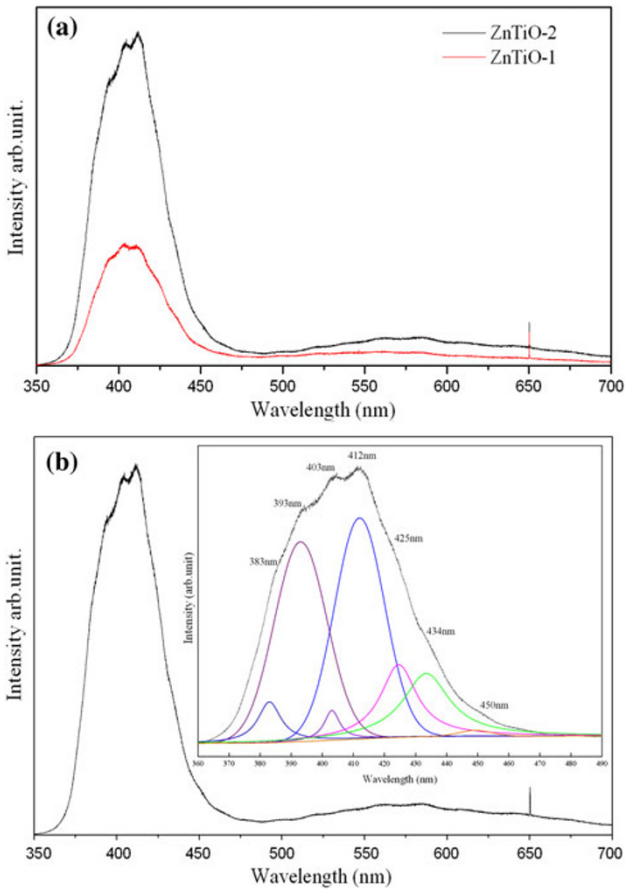

Fig. 6 **a** Room temperature PL spectra of the ZnTiO-1 and ZnTiO-2 porous films with a 325 nm laser source, and **b** fitted curves of ZnTiO-2 porous film

solution without any catalyst increased slowly over the time period. This could be resulted from the evaporation of water in the solution, which decreased the total volume of the solution. Even though the absolute amount of estrone did not change, the appeared concentration was raised.

With ZnO porous film as photocatalyst, estrone concentration kept decreasing over the 4 h period and more than 60% of estrone was degraded at the end of UV irradiation. The estrone degradation curve catalyzed by ZnTiO-1 has the same trend to that with the ZnO catalyst and slightly lower, indicating the porous film has better photocatalytic performance. However, the difference between these two curves (33 vs. 38% at 240 min) is not large enough to tell whether it is caused by the addition of TiO_2. It could be due to the amount of TiO_2 being too small.

The ZnTiO-2 porous films were then tested for photocatalytic activity under UV irradiation together with the ZnO porous film. The test setup was the same as before, and the results are shown in Fig. 8, exhibiting similar results as those in Fig. 7. The catalytic efficiencies of these two films are at the same level, again the film ZnTiO-2 has a slightly better performance, but the difference is not significant.

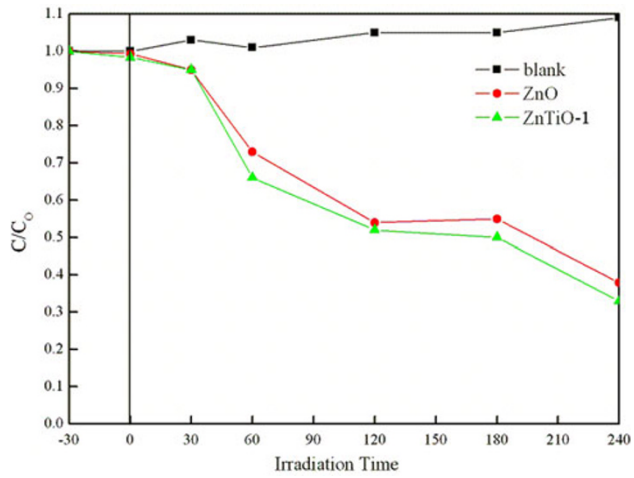

Fig. 7 Concentration profiles of estrone solution showing estrone degradation kinetics under UV irradiation without catalyst (*black line*), with ZnO porous film as catalyst (*red line*), and with porous film ZnTiO-1 as catalyst (*green line*)

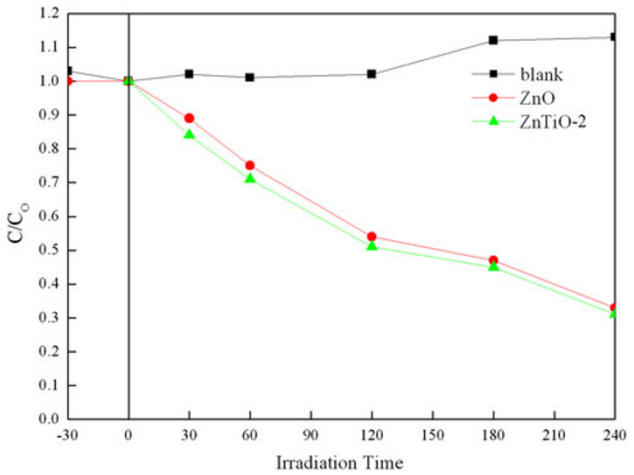

Fig. 8 Concentration profiles of estrone solution under UV irradiation without catalyst (*black line*), with ZnO porous film as catalyst (*red line*), and with porous film ZnTiO-2 as catalyst (*green line*)

It should be noted that the wavelength of the UV light is 365 nm, so the photo energy is higher than the band gap of both ZnO and TiO_2. One of the possible advantages of the ZnO–TiO_2 porous film, however, is the absorption of visible light demonstrated by the UV-VIS and PL test, which cannot be shown using this UV light source. Therefore, this test can only demonstrate that ZnO and ZnO–TiO_2 porous films have slightly better but similar photocatalytic abilities under UV light.

UV-VIS degradation

The catalytic performance of ZnO and film ZnTiO-1 was then tested under UV-VIS light source. The experiment

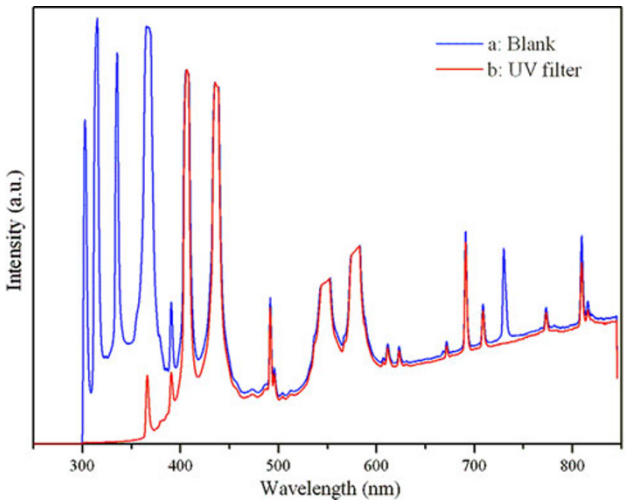

Fig. 9 **a** The incident light spectrum on the solution surface: Curve (*a*) measured without a filter, and Curve (*b*) measured with a UV filter

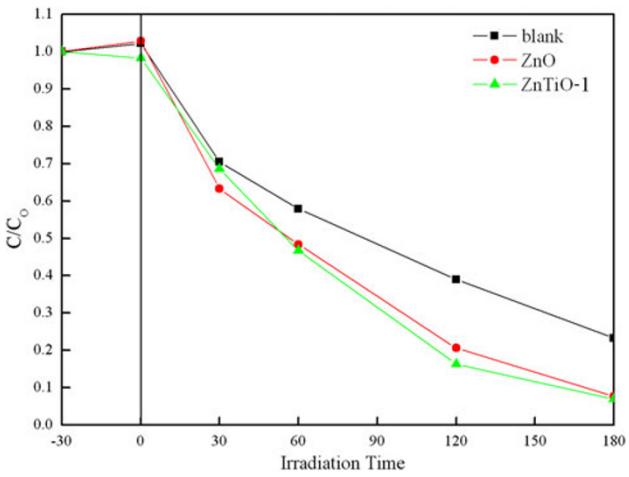

Fig. 10 Concentration profiles of estrone solution under UV-VIS light irradiation without catalyst (*black line*), with ZnO porous film as catalyst (*red line*), and with ZnTiO-1 porous film as catalyst (*green line*)

setup and test procedure were the same as the previous one, but the degradation time was changed to 3 h. The incident light intensity on the solution surface was measured, and the Curve (a) in Fig. 9 with blue colour shows the measured light spectrum.

Figure 10 illustrates the test results. Without the presence of porous films, the estrone concentration also went down in the 3 h period. Estrone was known can be decomposed under short wavelength UV light ($\lambda = 254$ nm) (Liu and Liu 2004). Although the spectrum of the incident light [Curve (a) in Fig. 9] does not shown any light intensity below 300 nm, that could be due to the insensitivity of the radiometer for light with wavelength below 300 nm. The UV-VIS may also emit UV light with wavelength lower than 300 nm. Thus, the estrone concentration reduction in the blank solution could be resulted from the direct photolysis of estrone.

However, with ZnO and ZnO–TiO_2 film as photocatalysts, estrone concentration decreased rapidly and more than 90% of the estrone had been degraded at the end of the 3 h UV-VIS irradiation. These result shows that the ZnO–TiO_2 porous film has good photocatalytic behaviour in the UV-VIS light range, although the test results still do not give a big difference in the catalytic ability between ZnO and ZnO–TiO_2 films. This may be because the incident light has a large component of UV light, so the major degradation was caused by UV light, and thus the effect of the visible light became small.

Visible light degradation

One way to examine the effect of TiO_2 on the photocatalytic ability of the porous film is eliminating the UV light. Therefore, the photocatalytic activities of ZnO porous film, film ZnTiO-1 and ZnTiO-2 were tested under visible light, which was obtained by blocking the UV light of the lamp using a UV filter (Kenko). Curve (b) in Fig. 9 shows the light intensity distribution (in red) at the solution surface when the UV filter was used. Only two small UV peaks at 365 and 390 nm were left after the blocking, and the short wavelength UV light ($\lambda < 300$ nm) was completely eliminated. Hence, the photolysis of estrone would not occur in this test.

The test results are summarized in Fig. 11. Under visible light, the photocatalytic activity of ZnO porous film was reduced. After 4 h exposure time, about 35% of estrone was degraded by ZnO porous film. On the other hand, the TiO_2 containing porous film showed a much better

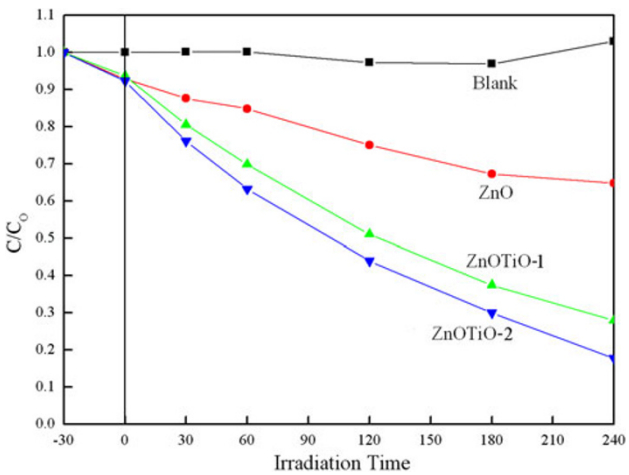

Fig. 11 Concentration profiles of estrone solution under visible light irradiation without catalyst (*black line*), with ZnO porous film as catalyst (*red line*), with porous film ZnTiO-1 as catalyst (*green line*), and with porous film ZnTiO-2 as catalyst (*blue line*)

photocatalytic performance than ZnO porous film under the visible light. After 4 h degradation, 72% estrone was decomposed in the solution with ZnTiO-1 as the catalyst, and the C/Co value in the solution containing film ZnTiO-2 was only around 17%. The higher catalytic activity of the latter one can be attributed to the higher TiO_2 content added by the sol-gel treatment. These results agree well with the optical properties found by UV-VIS and PL testing.

Conclusions

Highly porous ZnO and ZnO–TiO_2 composite films have been produced by reactive sputtering and wet oxidation method. The films can reach very high thickness (50 μm) with uniformly distributed porosity. The ZnO–TiO_2 film produced by the reactive co-sputtering Zn and TiO_2 targets followed by wet oxidation has a low TiO_2 composition and TiO_2 nano-clusters in anatase phase were formed on the surface of the film after the wet oxidation. The film produced from the routine of reactive sputtering Zn targets-wet oxidation-sol spin can increase the TiO_2 composition without much reduction in porosity. These porous ZnO–TiO_2 films showed enhanced PL spectrum in visible light range due to the resonant effect of TiO_2 with ZnO.

The photocatalytic abilities of these porous ZnO and ZnO–TiO_2 films have also been tested. Both ZnO and ZnO–TiO_2 porous films have good photo-degradation ability to estrone under UV and/or visible light. Their catalytic performances under UV light were similar, but were quite differences when under visible light. The TiO_2 containing porous films had much higher photocatalytic activity than ZnO porous film under visible light, which is attributed to the high surface area resulted from the porous structure and the existence of anatase phase TiO_2.

Acknowledgments The authors would like to thank KACST for the partial support from the project No. 237-29, and Department of Chemical & Materials Engineering, the University of Auckland for various support and assistance.

References

Baltazar P, Lara V, Córdoba G, Arroyo R (2006) Kinetics of the amorphous—anatase phase transformation in copper doped titanium oxide. J Sol-Gel Sci Technol 37(2):129–133

Bavykin DV, Friedrich JM, Walsh FC (2006) Protonated titanates and TiO_2 nanostructured materials: synthesis, properties, and applications. Adv Mater 18(21):2807–2824

Choi WS, Kim EJ, Seong SG, Kim YS, Park C, Hahn SH (2009) Optical and structural properties of ZnO/TiO_2/ZnO multi-layers prepared via electron beam evaporation. Vacuu 83(5):878–882

Gan X, Li X, Gao X, He X, Zhuge F (2009) Deposition potential dependence of ZnO-eosin Y hybrid thin films prepared by electrochemical deposition and their photoelectrochemical properties. Mater Chem Phys 114(2–3):920–925

Gong D, Grimes CA, Varghese OK, Hu W, Singh RS, Chen Z, Dickey EC (2001) Titanium oxide nanotube arrays prepared by anodic oxidation. J Mater Res 16(12):3331–3334

Hulteen JC, Martin CR (1997) A general template-based method for the preparation of nanomaterials. J Mater Chem 7(7):1075–1087

Hsu YF, Djurišić AB, Tam KH, Cheung KY, Chan WK (2007) Fabrication and characterization of ZnO/TiO_2 nanoscale heterojunctions. J Cryst Growth 307(2):348–352

Lee JC, Park KS, Kim TG, Choi HJ, Sung YM (2006) Controlled growth of high-quality TiO_2 nanowires on sapphire and silica. Nanotechnology 17(17):4317–4321

Lei Y, Zhang LD, Meng GW, Li GH, Zhang XY, Liang CH, Chen W, Wang SX (2001) Preparation and photoluminescence of highly ordered TiO_2 nanowire arrays. Appl Phys Lett 78(8):1125–1127

Liu B, Liu X (2004) Direct photolysis of estrogens in aqueous solutions. Sci Total Environ 320(2–3):269–274

Liu P, Li W, Zhang J (2009) Electrodeposition and photocatalytic selectivity of ZnO/Methyl blue hybrid thin films. J Phys Chem C 113(32):14279–14284

Luque A, Hegedus S (2003) Handbook of photovoltaic science and engineering. Wiley, Hoboken

Mardare D, Tasca M, Delibas M, Rusu GI (2000) On the structural properties and optical transmittance of TiO_2 r.f. sputtered thin films. Appl Surf Sci 156(1–4):200–206

Masaru Y, Ken H, Osamu Y (1997) Formation and sintering of TiO_2 (Anatase) solid solution in the system TiO_2–SiO_2. J Am Ceram Soc 80(10):2749–2753

Nakajima H, Mori T, Shen Q, Toyoda T (2005) Photoluminescence study of mixtures of anatase and rutile TiO_2 nanoparticles: influence of charge transfer between the nanoparticles on their photoluminescence excitation bands. Chem Phys Lett 409(1–3):81–84

Saraf LV, Patil SI, Ogale SB, Sainkar SR, Kshirsager ST (1998) Synthesis of nanophase TiO_2 by ion beam sputtering and cold condensation technique. Int J Mod Phys B 12(25):2635–2647

Vogel D, Krüger P, Pollmann J (1995) Ab initio electronic-structure calculations for II–VI semiconductors using self-interaction-corrected pseudopotentials. Phys Rev B 52(20):R14316

Wu JM, Shih HC, Wu WT, Tseng YK, Chen IC (2005) Thermal evaporation growth and the luminescence property of TiO_2 nanowires. J Cryst Growth 281(2–4):384–390

Xi YY, Hsu YF, Djurisic AB, Chan WK (2008) Electrochemical synthesis of ZnO nanoporous films at low temperature and their application in dye-sensitized solar cells. J Electrochem Soc 155(9):D595–D598

Zou CW, Yan XD, Han J, Chen RQ, Bian JM, Haemmerle E, Gao W (2009) Preparation and enhanced photoluminescence property of ordered ZnO/TiO_2 bottlebrush nanostructures. Chem Phys Lett 476(1–3):84–88